Journal of the Ceramic Society of Japan 116 [1] 100-104 2008 Paper

TEM observation of hydroxyapatite nanocrystals ionically-bonded onto the graftpolymer-modified PET substrate

Atsutomo NAKAMURA, Atsumasa SHISHIDO, Ippei KISHIDA, Masahiro OKADA,* Tsutomu FURUZONO* and Yoshiyuki YOKOGAWA

Graduate School of Mechanical and Physical Engineering, Osaka City University, 3-3-138 Sugimoto, Sumiyoshi-ku, Osaka 558-8585
***Department of Bioengineering, National Cardiovascular Center Research Institute, 5-7-1 Fujishiro-dai, Suita, Osaka 565-8565**

The crystallographic orientation relationship between hydroxyapatite (HAp) nanocrystals and poly (acrylic acid) (PAA) graftpolymer-modified poly (ethylene terephthalate) (PET) substrate was studied using transmission electron microscopy (TEM). We observed the microstructure of fabricated rod-like HAp nanocrystals and the interface of HAp/PET composite where, the HAp nanocrystals are bonded onto PAA graftpolymer-modified PET substrate. The selected-area electron diffraction (SAED) pattern of interface of the HAp/PET composite indicated that some low index planes in HAp prism plane tended to be contact plane with the PET substrate surface. In particular, the $\{11\bar{2}0\}$ plane was distinctly found as the contact plane with PET substrate. In this material, it has been reported that the carboxyl groups of PAA graft-polymer are ionically-bonded with Ca ions on surface of the HAp nanocrystal. It was suggested that the periodic ionic arrangements of the $\{11\bar{2}0\}$ plane play an important role on the bonding between the HAp nanocrystals and the carboxyl groups of graft-polymer on the PET substrate.

Key-words : Hydroxyapatite, Composite, Biomaterial, Interface, Transmission electron microscopy

[Received October 12, 2007; Accepted December 11, 2007] @2008 The Ceramic Society of Japan

1. Introduction

Hydroxyapatite (HAp; $Ca_{10}(PO_4)_6(OH)_2$) is one of main components of human bone and tooth. Artificially synthetic HAp ceramics are therefore widely used as biomedical materials due to its superior biocompatibility to human body.[1),2)] To improve the biocompatibility of many medical devices used in human body, for example, the coating of artificially synthetic HAp onto the surface of medical devices has been done.[2)-5)] Most of the HAp coatings has been used on a hard substrate.[1),2)] Recently, a new fabrication method of the composite using the HAp nanocrystals ionically-bonded onto the soft polymers such as silk fibroin and poly (ethylene terephthalate) (PET) was developed.[4)-7)] It was reported that the HAp/PET composite has an advantage of biological safety for the infection, compared with the composite using a protein such as collagen derived from animal.[5)] Thus, the HAp/PET composite has potential applications of percutaneous medical devises such as percutaneous dialysis catheter and artificial blood vessel.

The biocompatibility of the HAp composite is considered to be closely related to the covering ratio of HAp nanocrystals on the substrate surface of the composite, but little is known about the interface between the HAp nanocrystals and the polymer substrate. For the further improvement of the biocompatibility, it will be needed to clarify the interface structure in detail.

While biological and chemical properties of the HAp/PET composite have been studied intently, crystallographic study of the interface has never been reported. In the previous studies, surface morphology of the composite were observed by scanning electron microscopy (SEM),[6)] and the evidence that the ionic bond were formed between the HAp nanosrystals and graftpolymer were confirmed by FT-IR mesurements.[7)] However, the crystallographic orientation relationships have been not determined. In the present study, therefore, in order to investigate the orientation relationship between the HAp nanocrystals and the poly (acrylic acid) (PAA) graftpolymer-modified PET substrate, the interface was observed by transmission electron microscopy (TEM). The electron diffraction patterns including selected-area electron diffraction (SAED) pattern were analyzed in detail.

2. Experimental

The HAp nanocrystals were fabricated by a wet chemical process and were calcinated at 800°C for 1 h using an anti-sintering agent to prevent the calcination-induced sintering among the nanocrystals.[8)] The anti-sintering agent, calcium salt of poly (acrylic acid) (PAA-Ca), was coated on the nanocrystals before calcination, by adding $Ca(OH)_2$ supersaturated solution into an aqueous dispersion of the HAp nanocrystals adsorbed by poly (acrylic acid) (PAA). As a result, PAA-Ca precipitated on the nanocrystal surfaces. Although the organic component of PAA-Ca was thermally decomposed during calcination, the decomposed product (CaO) remained on the crystals and prevented the contact among the crystals.[8)] After calcination, CaO was removed by washing with water. As-prepared and post-calcinated HAp nanocrystals were characterized using XRD and FT-IR measurements in previous study.[8)]

HAp/PET composite was fabricated by the following process shown in **Fig. 1**. Firstly, a PAA-grafted PET substrate was prepared by the corona-discharge treatment followed by the graft polymerization of acrylic acid on the PET substrate at 60°C for 30 min.[3)] The PAA-grafted PET substrate was immersed in the HAp suspension in ethanol for 1 h at room temperature. The HAp/PET composite was washed with ethanol in an ultrasonic bath, and dried in air. Biological properties of HAp/polymer composite have been

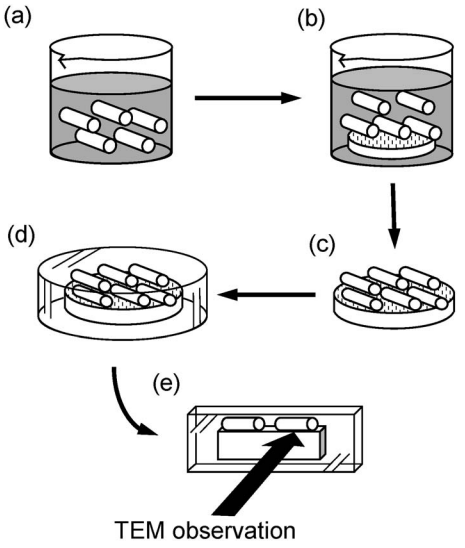

Fig. 1. Sample preparation of the HAp/PET composite for TEM observation. (a) Aqueous suspension of HAp nanocrystal with ethanol solution. (b) The PAA-grafted PET substrate was immersed in the HAp suspension in ethanol for 1 h at room temperature. (c) The HAp/PET composite was washed with ethanol in an ultrasonic bath, and dried in air. (d) The composite was embedded with resin. (d) After the composite was cut out to form an ultra-thin section by a conventional microtoming, the composite interface was observed by TEM.

reported in elsewhere.[4)-7)]

The HAp nanocrystals were characterized by TEM in order to confirm its morphology and crystallography. For the TEM observation, the HAp nanocrystals dispersed in methanol solution were dripped onto the carbon foils supported by copper grids and then they were dried. Also, the HAp/PET composites were observed to investigate the orientation relationship between the HAp nanocrystals and the graftpolymer-modified PET substrate. As shown in Fig. 1, after embedding with resin, the composite was cut out to form an ultra-thin section by a conventional microtoming. TEM observation in this study were performed using a conventional TEM (JEM-2100, JEOL) operated at 200 kV. In order to avoid charging problem during TEM observation, amorphous carbon was deposited onto the sample surface.

It had been believed that the HAp crystal structure had a hexagonal symmetry with the space group $P6_3/m$.[9)] However, it was confirmed that stoichiometric HAp has a monoclinic symmetry in a subsequent study.[10)] In this study, we selected to express the HAp crystal structure with a hexagonal Miller index according to the hexagonal symmetry, because its structure can be mostly explained with hexagonal symmetry. **Figure 2** is a schematic of [0001] structure of HAp using hexagonal symmetry. Generally, the hexagonal symmetry has two typical prism planes of $\{1\bar{1}00\}$ and $\{11\bar{2}0\}$. Translation distances along the $[1\bar{1}00]$ and $[11\bar{2}0]$ directions of the HAp structure were 0.81 nm and 0.94 nm, respectively.[9)] The $\{1\bar{1}00\}$ plane has an angular-difference of 30 or 90 degrees to the $\{11\bar{2}0\}$ plane around the [0001] axis.

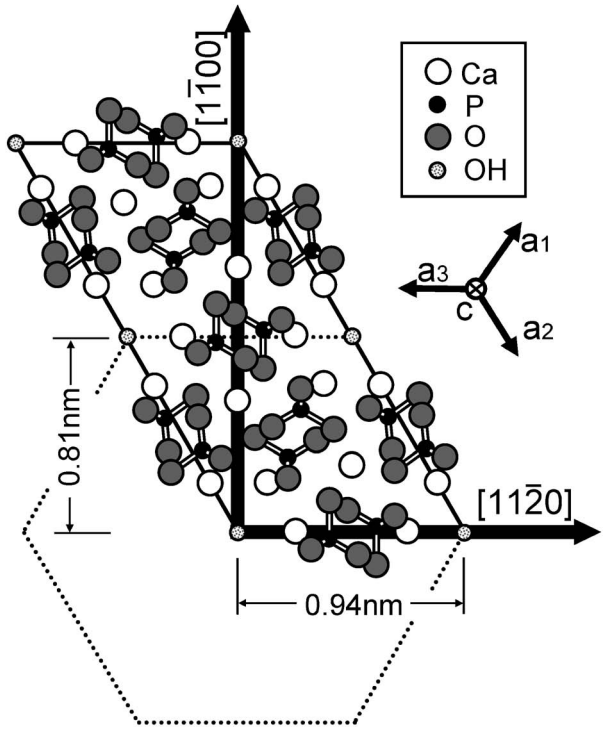

Fig. 2. Schematic of the [0001] structure of HAp crystal using hexagonal symmetry. There are two typical low index planes of $\{1\bar{1}00\}$ and $\{11\bar{2}0\}$. Translation distances along the $[1\bar{1}00]$ and $[11\bar{2}0]$ directions of HAp structure are 8.1 Å and 9.4 Å, respectively.[9)] The $\{1\bar{1}00\}$ plane has an angular-difference of 30 or 90 degrees to the $\{11\bar{2}0\}$ plane around the [0001] axis.

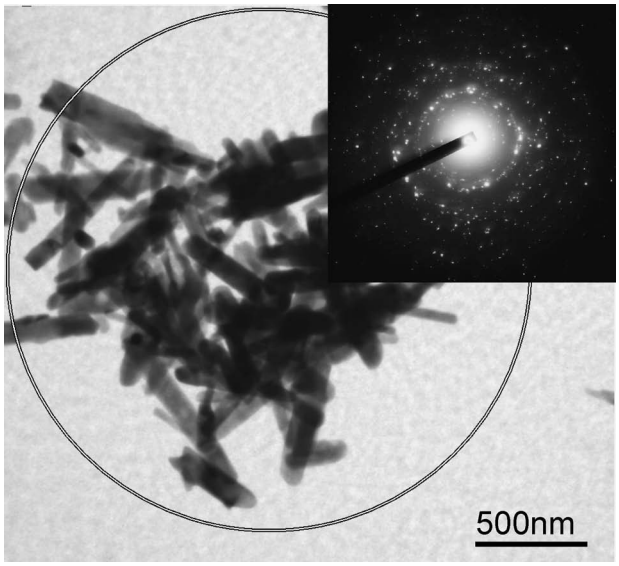

Fig. 3. A bright field image of HAp nanocrystals and its SAED pattern. The circle on the bright field image corresponds to the range of SAED pattern. It can be seen that the nanocrystals were formed into agglomerates.

3. Results and discussion

3.1 TEM observation of fabricated HAp nanocrystals

Figure 3 shows a TEM bright field image and its SAED

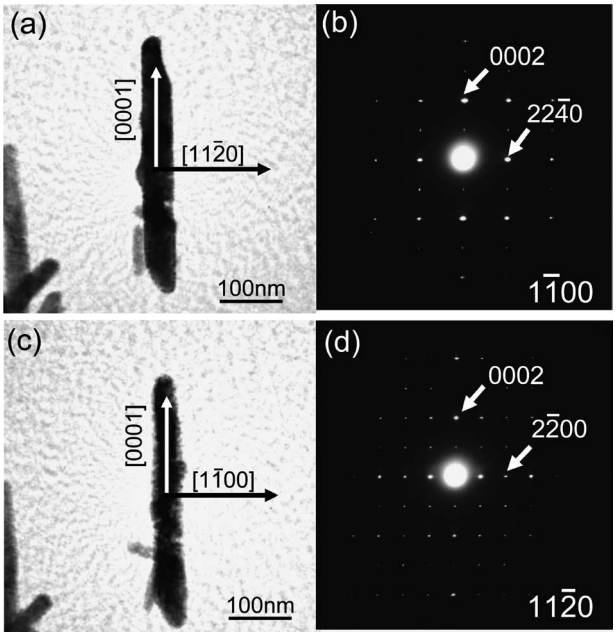

Fig. 4. Bright field images of an isolated HAp nanocrystal and their SAED patterns. The image in (c) was derived from (a) by tilting the same sample at 30 degrees around the [0001] axis. The SAED patterns in (b) and (d) are from (a) and (c), which correspond to the [1$\bar{1}$00] and [11$\bar{2}$0] zone axes of HAp structure, respectively.

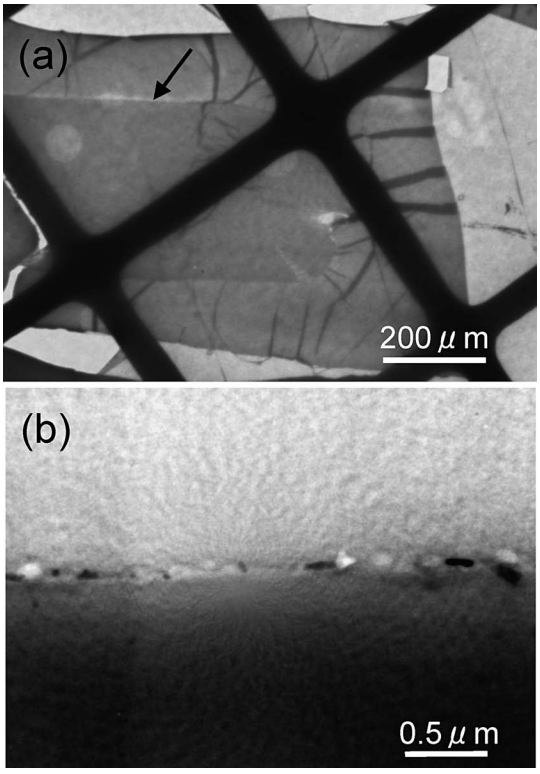

Fig. 5. Bright field images of HAp/PET composite in low magnification. The image in (a) shows that the sample was embedded with resin as an ultra-thin section, while that in (b) shows a slightly magnified image of the area arrowed in (a).

pattern. As can be seen in this figure, the rod-like nanocrystals with the diameter of 10–100 nm were often formed into agglomerates, although individual nanocrystals were separated before the preparation of TEM foil. This is considered due to a capillary force during evaporation of the medium in dripping onto the carbon foil for TEM observation. As can be seen in this figure, SAED patterns of agglomerates were spotty dispersed. This indicates a slight difference in lattice parameters among each crystal. It has been widely reported that the structure and properties of the HAp are dependent on the degree of the carbonate substitution during the thermal treatment in CO_2 containing atmosphere.[11),12)] Therefore, the dispersed diffraction pattern shown in Fig. 3 may be due to a deviation on the development of the carbonate substitution in calcination process.

Figures 4(a) and (c) shows the bright field images of an isolated HAp nanocrystal. Fig. 4(c) was derived from Fig. 4 (a) by tilting the same sample at 30 degrees around the [0001] axis. Fig. 4(b) and (d) show the SAED patterns from Fig. 4(a) and (c), which correspond to the [1$\bar{1}$00] and [11$\bar{2}$0] zone axes of HAp structure, respectively. It was found that the long axis direction corresponded to the [0001] direction. This character has been commonly reported for the HAp crystal synthesized with aqueous system.[8),13)] As can be seen in the SAED patterns, the HAp nanocrystals are not polycrystal or amorphous but an absolute single-crystal, although SAED pattern from agglomerates were spotty dispersed.

3.2 TEM observation of interface of HAp/PET composite.

Figure 5 shows the bright field images of the HAp/PET composite sample in low magnification. As can be seen in Fig. 5(a), the sample was embedded with resin as an ultra-thin section. Fig. 5(b) shows a slightly magnified image of the area arrowed in Fig. 5(a). It was confirmed that the HAp nanocrystals were present on the surface of the PET substrate.

Figure 6 shows a TEM bright field image obtained from around the interface of a HAp/PET composite with a corresponding SAED pattern taken along the [1$\bar{1}$00] zone axis. In this case, the tilting condition of *x*-axis and *y*-axis in TEM were -2.1 and -7.5 in degrees, respectively. Owing to the very weak contrast between PET substrate and embedding resin, there was a difficulty in confirming whether the interface is parallel to incident beam or not. In this point, we assumed that the interface is almost parallel to the incident beam direction without any tilting, since all samples were cut out by using a microtome in order that its cutting face should be perpendicular to the interface of the composite. On the basis of the SAED patterns, it was confirmed that the long axis direction that corresponds to the [0001] direction of the HAp nanocrystal is parallel to the substrate surface. In addition, it was considered that the {11$\bar{2}$0} plane of the HAp nanocrystal was a contact plane with the PET substrate surface in the case of Fig. 6. Here, the above tilting was conducted because the long axis directions are random on the PET substrate.

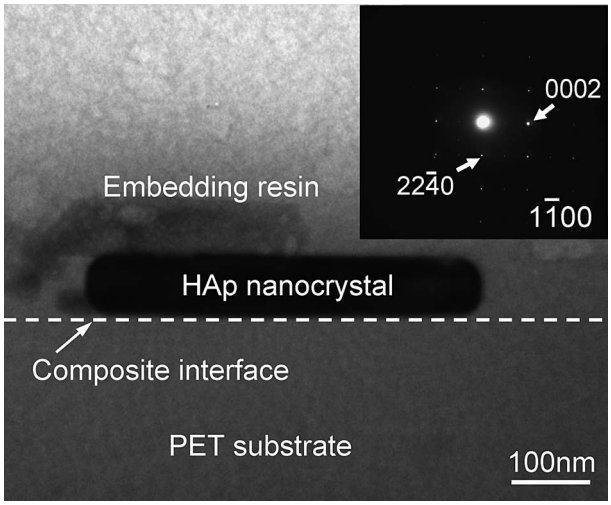

Fig. 6. Bright field image and its SAED pattern of HAp/PET composite interface. On the basis of the comparison with SAED pattern, it was confirmed that the long axis direction that corresponds to the [0001] direction of the HAp nanocrystal is parallel to the substrate surface. In addition, it was considered that the $\{11\bar{2}0\}$ plane of the HAp nanocrystals was a contact plane with the PET substrate surface. Here, the tilting condition of x-axis and y-axis in TEM sample stage were -2.1 and -7.5 in degrees, respectively.

Table1. Crystallographic Orientation Relationship in the Interface of HAp/PET Composite. Sample 1 in the Table Corresponds to Fig. 6. Tilting *x* and *y* in the Table Correspond to *x*- axis and *y*-axis on Sample Stage of TEM, Respectively

Sample number	Incident beam direction	**Contact plane with PET**	(Tilting x [degrees])	(Tilting y [degrees])
1	$[1\bar{1}00]$	$\{11\bar{2}0\}$	-2.1	-7.5
2	$[1\bar{1}00]$	$\{11\bar{2}0\}$	7.8	-1.0
3	$[1\bar{1}00]$	$\{11\bar{2}0\}$	-4.7	-0.3
4	$[1\bar{1}00]$	$\{11\bar{2}0\}$	1.5	-3.2
5	$[1\bar{1}00]$	$\{11\bar{2}0\}$	6.0	-3.5
6	$[1\bar{1}00]$	$\{11\bar{2}0\}$	5.8	-2.3
7	$[1\bar{1}00]$	$\{11\bar{2}0\}$	1.5	1.0
8	$[1\bar{1}00]$	$\{11\bar{2}0\}$	-3.1	-3.1
9	$[4\bar{5}10]$	$\{21\bar{3}0\}$	2.4	-2.6
10	$[4\bar{5}10]$	$\{21\bar{3}0\}$	4.2	-2.4
11	$[11\bar{2}0]$	$\{1\bar{1}00\}$	0.3	-0.3
12	$[11\bar{2}0]$	$\{1\bar{1}00\}$	3.5	-2.1
13	$[11\bar{2}0]$	$\{1\bar{1}00\}$	13.8	-1.0
14	$[11\bar{2}0]$	$\{1\bar{1}00\}$	9.1	2.5

The crystallographic orientation relationships obtained in this study are shown in **Table 1**. It can be seen that the various low index planes were found as a contact plane with the PET substrate surface in the relatively low tilting condition. In particular, the $\{11\bar{2}0\}$ planes were distinctly found as the contact plane with PET substrate. In addition, since the $[4\bar{5}10]$ direction in the sample 9 and 10 is close to the $[1\bar{1}00]$ direction in this table, their contact planes with the PET substrate may be the $\{11\bar{2}0\}$ plane, too. In the case of just two samples 11 and 12, the contact plane seemed to be the $\{1\bar{1}00\}$ plane.

Because an ionic bond formed by the reaction between the Ca ions on HAp crystal and the carboxyl groups of the graftpolymer on the PET substrate,[7] the location of the ions on HAp crystal surface is important for the orientation relationship. In the low index plane of the HAp prism plane, the ions such as Ca and OH groups were arranged with regularity and periodicity. Therefore, it is considered that the low index plane can play an important role on the ionic bonding. It is reported that the HAp crystals are often facetted with the $\{1\bar{1}00\}$ plane, and that the plane reacts with the carboxyl groups.[14),15)] In this study, however, not the $\{1\bar{1}00\}$ plane but the $\{11\bar{2}0\}$ plane seemed to be dominant as a contact plane with PET substrate surface as can be seen in Table 1. Here, note that the surface of HAp nanocrystals was modified with PAA-Ca using a PAA in $Ca(OH)_2$ aqueous solution to prevent the calcination-induced sintering. Therefore, it was considered that the surface of HAp nanocrystals might be modified with residual Ca ions. That is, the surface modification of HAp nanocrystals may bring about unusual bonding reaction with the PET substrate. It is interesting that the low index planes with regular and periodic atomic arrangements play an important role on the ionic bond to the substrate.

4. Summary

We observed the microstructure of rod-like HAp nanocrystals and the interface of HAp/PET composite, where the HAp nanocrystals were bonded onto PAA graftpolymer-modified PET substrate using transmission electron microscopy. The conclusion in this study can be summarized as follows.

(1) The SAED patterns from the agglomerates of rod-like HAp nanocrystals were spotty dispersed. This may be related to a deviation on the development of the carbonate substitution in calcination process.

(2) The SAED patterns from an isolated rod-like HAp nanocrystal indicated that the HAp nanocrystal was not polycrystal or amorphous but an absolute single-crystal, although SAED pattern from agglomerates were spotty dispersed. It was confirmed that the long axis direction of the HAp nanocrystals corresponded to the [0001] direction of HAp structure.

(3) On the basis of the SAED patterns from the interface of HAp/PET composite, it was confirmed that the [0001] direction of rod-like HAp nanocrystals is parallel to the substrate surface. It was found that the $\{11\bar{2}0\}$ plane of the HAp nanocrystals tended to be a contact plane with the PET substrate surface of the composite. It was suggested that the $\{11\bar{2}0\}$ planes with regular and periodic ionic arrangements of the HAp nanocrystal can play an important role on the ionic bonding to the carboxyl groups of PAA graft-polymer on the PET substrate.

Acknowledgements We thank Ms. Naoko Uchida for her technical support in the present study. A part of this study was financially supported by Japan Society for the Promotion of Science, Japan.

References

1) T. Kokubo, H. M. Kim and M. Kawashita, *Biomater.*, 24, 2161–2175 (2003).
2) P. Ducheyne, W. Vanraemdonck, J. C. Heughebaert and M. Heughebaert, *Biomater.*, 7, 97–103 (1986).
3) T. Furuzono, K. Sonoda and J. Tanaka, *J. Biomed. Mater. Res.*, 56, 9–16 (2001).
4) T. Furuzono, J. Tanaka and A Kishida, *J. Mater. Sci. Mater. Med.*, 15, 19–23 (2004).

5) T. Furuzono, P. L. Wang, A. Korematsu, K. Miyazaki, M. Oidomori, Y. Kowashi, K. Ohura, J. Tanaka and A. Kishida, *Journal of Biomedical Material Research Part B: Appl. Biomater.*, 65B, 217–226 (2003).
6) T. Furuzono, M. Masuda, M. Okada, S. Yasuda, H. Kadono, R. Tanaka and K. Miyatake, *ASAIO J.*, 52, 315–320 (2006).
7) A. Korematsu, T. Furuzono, S. Yasuda, J. Tanaka and A. Kishida, *J. Mater. Sci. Mater. Med.*, 16, 67–71 (2005).
8) M. Okada and T. Furuzono, *J. Nanopar. Res.*, 9, 807–815 (2007).
9) I. Kay, R. A. Young and A. S. Posner, *Nature*, 204, 1050–1052 (1964).
10) J. C. Elliot, P. E. Mackie and R. A. Young, *Science*, 180, 1055–1057 (1973).
11) R. Z. Legeros, *Nature*, 205, 403–404 (1965).
12) I. R. Gibson and W. Bonfield, *J. Biomed. Mater. Res.*, 59, 697–708 (2002).
13) E. I. Suvorova and P. A. Buffat, *J. Microscopy*, 196, 46–58 (1999).
14) K. Sato, Y. Suetsugu, J. Tanaka, S. Ina and H. Monma, *J. Colloid interface Sci.*, 224, 23–27 (2000).
15) K. Sato, T. Kogure, Y. Kumagai and J. Tanaka, *J. Colloid interface Sci.*, 240, 33–138 (2001).